

Low-Complexity Space-Time Processor for DS-CDMA Communications

Javier Ramos, Michael D. Zoltowski, *Fellow, IEEE*, and Hui Liu, *Member, IEEE*

Abstract—A novel wideband beamforming technique for cellular CDMA systems is presented in this paper. The proposed algorithm asymptotically provides the maximum SINR estimate of the signal with the desired code (SDC) by optimally combining desired signals from different paths and canceling strong multiuser access interference (MUAI). A two-dimensional (2-D) matched filter structure is used where not only different temporal samples of the matched filter output are processed but where those from matched filters connected to different antenna are processed as well. In contrast to previously proposed techniques, an exact code synchronization for the SDC is not required. The algorithm presented herein asymptotically provides the arrival time of the multipaths within a bit period and the optimum beamformers for extracting each of them. Space-time filters for combining the fingers across both space and time while canceling the MUAI's are constructed correspondingly. The instrumental property exploited by this technique is the fact that although the respective spectra of the SDC and MUAI components at the matched filter output are statistically identical, the respective spectra of their squared values differ. A simplified RAKE structure-based receiver is also proposed. The 2-D RAKE receiver considerably decreases the computations but requires a coarse SDC code synchronization. A technique to achieve coarse SDC code synchronization is also proposed.

Index Terms—Adaptive antenna, CDMA, interference cancellation, multipath, RAKE.

I. INTRODUCTION

CODE-DIVISION multiple access (CDMA) possesses many intrinsic advantages over the earlier access techniques such as time-division multiple access (TDMA) and frequency-division multiple access (FDMA) [1]. However, it has fundamental difficulties in a near-far situation when transmission power from one user overwhelms signals of the others. In current practice, sophisticated power control schemes are often employed to maintain a balanced power distribution among the users. However, the full benefit of power control is exploitable only for stationary and slow-moving mobile stations.

Manuscript received December 8, 1998; revised July 2, 1999. This work was supported by the Air Force Office of Scientific Research under Grant F49620-95-1-0367, the National Science Foundation under Grant MIPS-9320890, and the Army Research Office's Focused Research Initiative under Grant DAAHO4-95-1-0246. The associate editor coordinating the review of this paper and approving it for publication was Prof. S. M. Jesus.

J. Ramos is with the Department of Telecommunications Engineering, Carlos III University of Madrid, Leganés, Spain (e-mail: javier@tsc.uc3m.es).

M. D. Zoltowski is with the School of Electrical Engineering, Purdue University, West Lafayette, IN 47907-1285 USA (e-mail: mikedz@ecn.purdue.edu).

H. Liu is with the Department of Electrical Engineering, University of Virginia, Charlottesville, VA 22903-2442 USA (e-mail: hliu@virginia.edu).

Publisher Item Identifier S 1053-587X(00)00083-0.

Adaptive antenna arrays provide an alternative means to cope with the near-far problem. By steering beams toward the desired user and decreasing the total MUAI's power level, system near-far resistance, i.e., immunity of the desired user's performance to power variations of the others, can be considerably enhanced. Besides alleviating the near-far problem, antenna arrays also increase the soft capacity of CDMA systems through interference suppression. Since, in CDMA communications, the system capacity is limited by interferences instead of the bandwidth as in TDMA [2], [3], the reduction in system noise floor due to spatially selective transmission and reception leads to a direct increase in capacity [4]. The ability to cancel strong MUAI's also permits a higher degree of cross-correlation among users' signature codes, thereby allowing more active users to coexist within a given cell [2], [4]–[14]. The redundancy provided by multiple antennas is also essential in combating multipath fading in a dynamic mobile environment. Other benefits of adaptive antennas include advances in operational parameters such as coverage range, power consumption, security, etc.

While adaptive antennas improve the performance of CDMA communications in space domain, a RAKE receiver attempts the same goal through temporal operations. Fig. 1 shows the structure of a RAKE receiver. The input signal is correlated (multiplied and lowpass filtered) with delayed replicas of the same *desired code*, and correlator outputs are subsequently combined to yield a signal estimate. The idea behind the RAKE receiver is to coherently combine multipath signals from the desired user to enhance the output signal-to-noise ratio (SNR) in a frequency selective fading environment (wideband CDMA). The effectiveness of RAKE receivers has been demonstrated by both theoretical and experimental studies [15]. However, because the SDC and MUAI's have the same spectrum, time-only processing techniques can only suppress MUAI's to a certain extent unless additional knowledge, such as the codes for the interferences, is assumed [16]–[19].

Recently, there has been an increasing interest in the use of 2-D RAKE to simultaneously exploit space and time diversities by combining adaptive antennas with RAKE receivers. In principle, a 2-D RAKE receiver allows constructive combination of multipath signals received by an array of antennas while minimizing the MUAI's contribution, thus providing an optimum output signal-to-interference-plus-noise ratio (SINR) for a desired user. The potential of the 2-D RAKE has been evaluated and proved by various studies [4], [10], [20].

Although theoretically sound, the implementation of 2-D RAKE is nontrivial in practice. Most of the previously developed 2-D RAKE receivers involve complicated spatial and

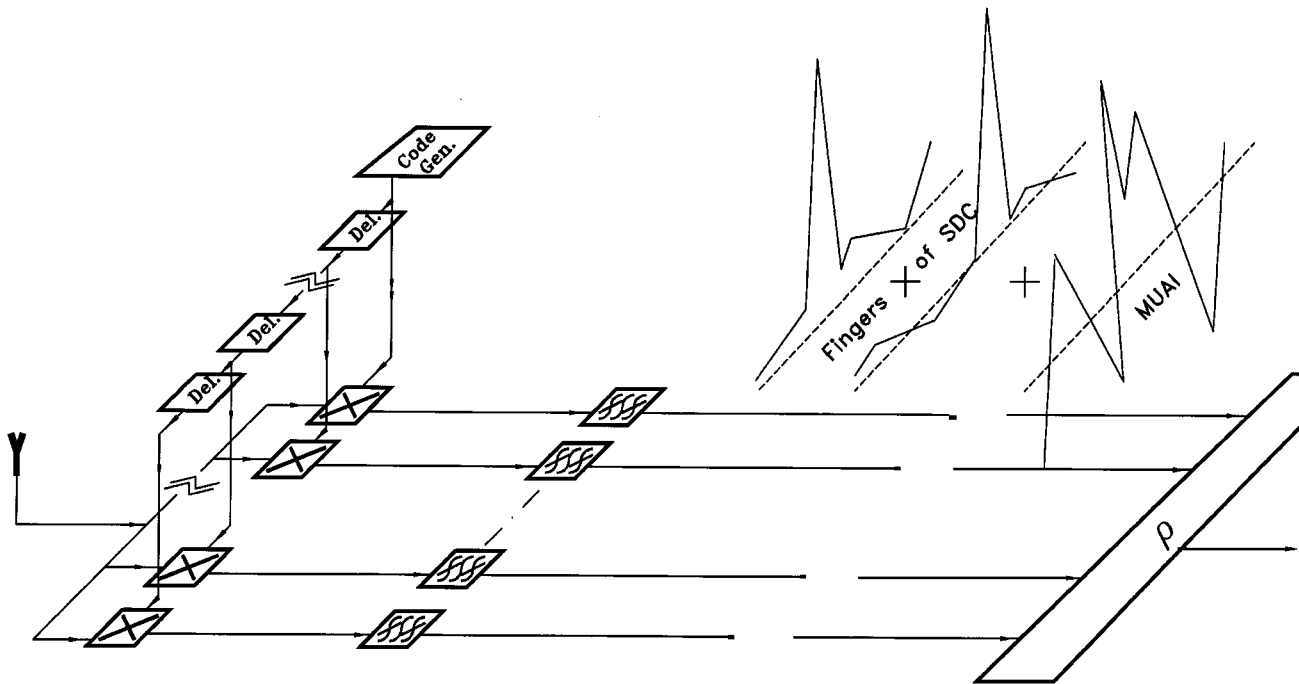


Fig. 1. RAKE receiver.

temporal operations, which may prohibit their applications in a fast varying environment. For example, the 2-D RAKE receiver proposed in [20] consists of a two-stage batch process; the parameters of the SDC multipaths, including direction-of-arrival (DOA) and relative delays of multipath signals, are estimated in the first stage, whereas the optimum spatial-temporal filter for combining the space-time samples is constructed in the second stage based on the parameter estimates obtained in the first stage. Because of a large number of measurements and the required array calibration for the DOA estimation, applicability of the algorithm to real-time systems is questionable.

The schemes presented in [4] and [10] relax the array calibration requirement by sampling and processing array output signals before and after the correlators. Nevertheless, the cost problem remains since sampling before the correlator implies wideband digital signals and correspondingly faster and more expensive analog-to-digital converters (ADC's). In addition, the algorithm proposed in [4] does not incorporate temporal processing and, thus, is suboptimum in terms of combining multipath signals. Although the approach in [10] deals with both spatial and temporal processing, it involves larger dimension matrices unaffordable in real-time equipment. The major drawback of these pre- and post-correlation approaches, however, is that they are valid only when the delay between consecutive branches of the RAKE receiver are longer than the chip length; otherwise, the noise structure before and after the correlators is different. Unfortunately, smaller delays among the RAKE receivers are usually necessary for better reliability and performance [12].

An adaptive algorithm that can deal with fractionally spaced samples is developed in [9] and [11]–[13], wherein matched filters are used instead of RAKE receivers. With coarse SDC code synchronization, two time periods are established for processing: one close to the finger interval and a second one away

from it. The proposed approaches overcome the need of sampling before and after the matched filter/correlator and are applicable to any multipath scenarios. However, the computations required may still be prohibitively high due to the implementation of the matched filter and manipulations of large dimension space-time or space-frequency covariance matrices.

In [8], we presented a technique that avoids the need for code synchronization and decreases drastically the computational cost. It performs the same space-time combination but only uses the time samples corresponding to the correlation peak or *fingers* (see Fig. 1), leading to much reduced matrix dimensions. This technique is further improved in [21], where a modified algorithm is developed to speed up the convergence for rapidly varying channels.

II. SIGNAL MODE

The scenario considered herein is that of J users in a CDMA system sharing a common frequency band. Different spreading signatures or pseudo noise (PN) codes achieve discrimination among users. In this case, the baseband signal transmitted from the k th user can be represented as

$$s_k(t) = \sum_{n=-\infty}^{\infty} b_k(n)c_k(t - nT_b) \quad (1)$$

where

- $b_k(n)$ n th symbol (bit) value;
- $c_k(t)$ code assigned to k th user;
- T_b bit period.

The code is composed by L_c chips of duration T_c . The ratio $L_c = T_b/T_c$ is an indication of the MUAI rejection capability. Superimposed signals from J users are collected by a base station antenna array with N elements. There is no constraint on either the antenna locations or their respective radiation patterns.

Standard narrowband approximation in array processing is assumed, implying that the array dimensions are much smaller than cT_c , where c is the propagation speed.

For an arbitrary period of time within which the optimal space-time combination is to be performed, the signal transmitted from the k th user ($1 \leq k \leq J$) arrives at the antenna array via L_k paths. The direct path of the k user is received with amplitude σ_k . The remaining $L_k - 1$ multipaths of the k th user are attenuated, and the phase is shifted by the complex number ρ_k^l , $2 \leq l \leq L_k$. Therefore, without loss of generality, it is assumed that $|\rho_k^1| = 1$ for the k th user. The l th path of the k th user arrives with a delay of τ_k^l and through a direction $\boldsymbol{\theta}_k^l$, where the boldface on $\boldsymbol{\theta}$ denotes the fact that no constraint on the relative location between antenna elements is assumed so that the direction is 2-D (azimuth and elevation), in general. Under the narrowband assumption, the 2-D angle $\boldsymbol{\theta}_k^l$ influences only the complex scale factors among antennas, which are characterized by the array manifold $\mathbf{a}(\boldsymbol{\theta}_k^l)$. All the above parameters (number of paths, angles of arrival, and time delays) are random variables because of the physics behind the radio propagation. However, if the convergence rate of the adaptive combiner is faster than the inverse of the multipath channel coherence time, the parameters L_k , σ_k , ρ_k^l , τ_k^l and manifold $\mathbf{a}(\boldsymbol{\theta}_k^l)$ can be approximated by constants. In any case, these parameters are unknown, and they have to be estimated in order to perform the space-time matched filtering. Using the above notation, the received signals from the antenna array can be represented in a vector form as

$$\mathbf{x}(t) = \sum_{k=1}^J \sigma_k \sum_{l=1}^{L_k} \rho_k^l \mathbf{a}(\boldsymbol{\theta}_k^l) s_k(t - \tau_k^l) + \mathbf{n}(t) \quad (2)$$

where $\mathbf{n}(t)$ is the noise vector containing i.i.d. (independent and identically distributed) Gaussian white noise entries; thus, $E[\mathbf{n}(t)\mathbf{n}^H(t)] = \sigma_n^2 \mathbf{I}$, where σ_n^2 is the noise power, and \mathbf{I} is the $N \times N$ identity matrix.

A. Nonperiodic Code

Equation (1) assumes that the code remains the same from bit to bit. However, the current IS-95 [22] standard and many other CDMA systems use different parts of a longer code for each bit. This longer code is also called scrambling code. We refer to these systems as nonperiodic. In this case, the signal sent by the k th user is given by

$$s_k(t) = \sum_{n=-\infty}^{\infty} b_k(n) c_k^{(n)}(t - nT_b) \quad (3)$$

where $c_k^{(n)}(t)$ is the part of the code the k th user sends out during the n th bit. Substituting (1) by (3), (2) also holds for the nonperiodic system.

There are basically two implementations for recovering the bit values at a CDMA receiver: the matched filter based in the code waveform $h(t) = c(-t)$ and the correlator. At this point, it is worth clarifying that although both implementations can provide the same signal estimates from a digital detection view

point, there is a subtle difference between them. The matched filter is a linear operator that maximizes the signal-to-white-noise ratio (SWNR) of only one of the output samples per bit; the number of samples at the input and output of the filter are exactly the same. On the other hand, the correlator provides an output signal for every $L_c S_c$ inputs, where L_c is the number of chips per bit, and S_c is the number of samples per chip. However, the correlator yields the same value as the matched filter at sampling point where the SWNR is maximized. Of course, to achieve the same result, the correlator needs to know the correct code synchronism. The RAKE receiver we refer to herein is essentially formed with T correlators where the code is progressively delayed. The RAKE receiver is capable of offering the optimum signal estimate as long as the T correlators span the multipath spread. Therefore, the RAKE receiver computational load is $L_c S_c / T$ smaller than the matched filter load.

In the next section, we adopt the matched filter approach for the sake of notation simplicity. A more practical approach using a RAKE receiver will be derived in Section IV. The properties exploited in the following algorithms are satisfied by both (1) and (3). Therefore, the transition from one to the other does not represent any complication. Moreover, the use of nonperiodic codes leads to better results due to the variability of the MUAI's components at the output of the matched filter/RAKE receiver. However, the simultaneous use of matched filter and nonperiodic code complicates the notation since the impulsive response of the matched filter for nonperiodic modulations is time varying [9].

III. SPACE-TIME BLIND PROCESSOR

Using the matched filter implementation in Fig. 2, the output signal from each antenna in (2) is passed through a filter with impulse response $h(t) = c_1(-t)$. Without loss of generality, we assume the signal enumerated as $j = 1$ is the desired user (the SDC). The signal vector defined by the bank of filters output is

$$\mathbf{y}(t) = \sum_{k=1}^J \sigma_k \sum_{l=1}^{L_k} \rho_k^l \mathbf{a}(\boldsymbol{\theta}_k^l) \sum_{n=-\infty}^{\infty} b_k(n) c_k(t - nT_b - \tau_k^l) * c_1(-t) + \mathbf{n}_y(t) \quad (4)$$

where the operator $*$ denotes convolution, and $\mathbf{n}_y(t)$ is an $N \times 1$ vector containing i.i.d. random processes obtained as the element-wise convolution $\mathbf{n}(t) * c_1(-t)$.

With regard to each of the terms in (4), it is noted that ideally PN codes should satisfy $c_k(t) * c_i(t) = \delta_{ki} \delta(t)$, where δ_{ki} is the Kronecker delta, and $\delta(t)$ is the Dirac delta function. If this condition was strictly satisfied, only L_1 terms in (4) would be nonzero, and they would take nonzero values for $t = \tau_k^l$, $1 \leq l \leq L_1$. These terms are referred to as *fingers*. However, perfect orthogonality among codes cannot be achieved for each and every arbitrary time delay with finite length codes. Thus, residual cross- and autocorrelation undesired terms arise in practical systems. These spurious terms can be stronger than the fingers when the MUAI is received with much higher power levels than the SDC; hence, we have the *near-far problem*.

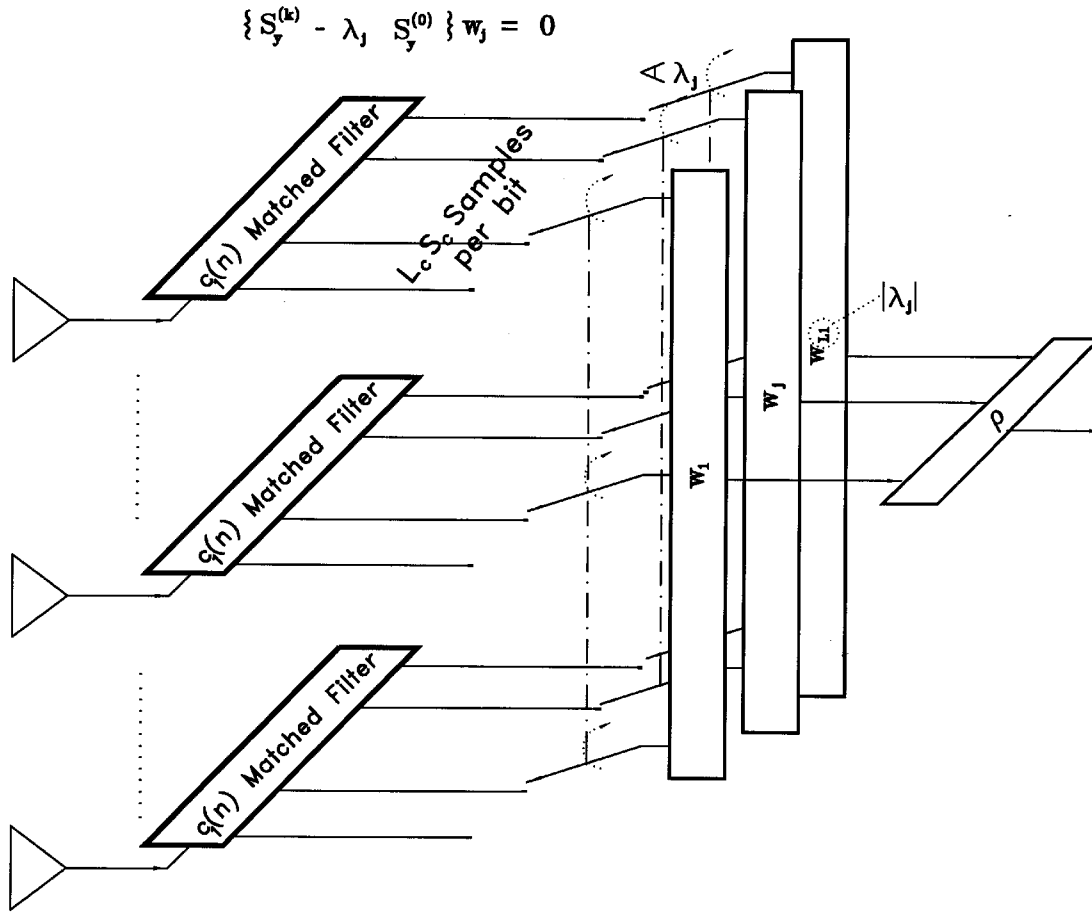


Fig. 2. Time-space matched filter.

A. Properties of Second-Order Statistics

Let the $N \times N$ time-varying correlation matrix $\mathbf{R}_y(t)$ be defined as

$$\mathbf{R}_y(t) \stackrel{\text{def}}{=} E \left[\mathbf{y}(t) \mathbf{y}^H(t) \text{rect} \left(\frac{t}{T_b} \right) \right] \quad (5)$$

where

- $E[\cdot]$ expectation operator;
- $(\cdot)^H$ conjugate transpose;
- $\text{rect}(t/T_b)$ unity over an interval of width T_b centered at $t = 0$ and zero elsewhere.

Further, let $\mathbf{S}_y(f)$ be defined as

$$\mathbf{S}_y(f) \stackrel{\text{def}}{=} \mathcal{F}[\mathbf{R}_y(t)] \quad (6)$$

where \mathcal{F} represents the element-wise Fourier transform operating on $\mathbf{R}_y(t)$.

Substituting the signal model in (4) and assuming: i) the symbol values are uncorrelated for a given user as well as between different users, i.e., $E\{b_k(n)b_p^*(m)\} = \sigma_b^2 \delta_{kp} \delta_{nm}$, where σ_b^2 is the average energy per symbol; ii) the noise is stationary, white (temporally uncorrelated) and i.i.d. (independent and identically distributed) for all the antennas with

variance σ_n^2 ; iii) noise is uncorrelated with all the user's signal; and iv) $c_k(t)$ are PN codes, (i.e., their FT $C_k(f)$ arguments are random variables uniformly distributed in $[0, 2\pi)$), the following proposition can be made:

Proposition:

$$\mathbf{S}_y(f) = \sum_{k=1}^J \sum_{l=1}^{L_k} p_k^l \mathbf{a}(\theta_k^l) \mathbf{a}^H(\theta_k^l) S_k^l(f) + \sigma_n^2 \mathbf{I} \text{sinc}(fT_b) \quad (7)$$

where

$$S_k^l(f) = \begin{cases} S_c(0)\delta(f), & \text{if } k \neq 1 \\ e^{j2\pi\tau_l f} S_c(f), & \text{if } k = 1 \end{cases} \quad (8)$$

$p_k^l = \sigma_k^2 |\rho_k^l|^2 \sigma_b^2$, $S_c(f) = [(|C_p(f)|^2 * |C_p(f)|^2) T(f)] \text{sinc}(fT_b)$, $C_p(f)$ is the Fourier transform of the chip pulse waveform, and $T(f) = \sum_{n=-\infty}^{\infty} e^{j2\pi f n T_b} = \sum_{n=-\infty}^{\infty} \delta(f - n/T_b)$.

Proof: See Appendix A.

In practical implementations, $\mathbf{R}_y(t)$ is computed from a sampled version of $\mathbf{y}(t)$ and $\mathbf{S}_y(f)$ as the DFT of $\mathbf{R}_y(n)$. Since $\mathbf{R}_y(t)$ is only nonzero for $-(T_b/2) \leq t \leq T_b/2$, the DFT of its sampled version evaluates $\mathbf{S}_y(f)$ at $f = \kappa/T_b$. We define

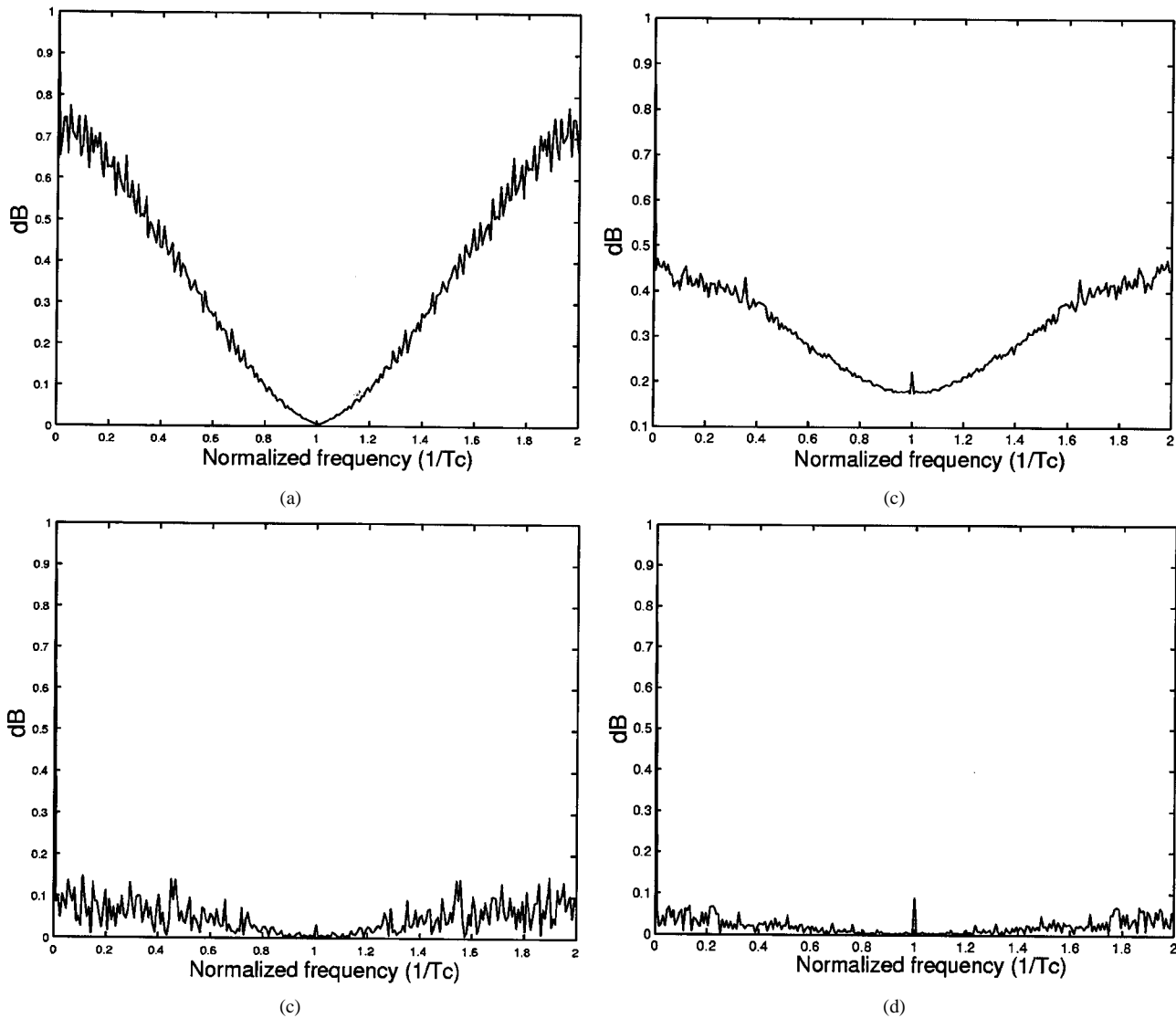


Fig. 3. $|S_k^l(\kappa)|$ for periodic code. (a) $k = 1$. (b) $k \neq 1$, nonperiodic code. (c) $k = 1$. (d) $k \neq 1$.

$S_y^{(\kappa)} = S_y(f)|_{f=\kappa/T_b}$. Substituting this definition in (7) results in

$$S_y^{(\kappa)} = \sum_{k=1}^J \sum_{l=1}^{L_k} \mathbf{a}(\theta_k^l) \mathbf{a}^H(\theta_k^l) P_k^l S_k^l \left(\frac{\kappa}{T_b} \right) + \sigma_n^2 \mathbf{I} \delta_{\kappa 0} \quad (9)$$

and similarly, $S_k^l(\kappa/T_b)$ gets the expression

$$S_k^l \left(\frac{\kappa}{T_b} \right) = \begin{cases} S_c(0) \delta_{\kappa 0}, & \text{if } k \neq 1 \\ e^{j2\pi\tau_1^l(\kappa/T_b)} S_c \left(\frac{\kappa}{T_b} \right), & \text{if } k = 1. \end{cases} \quad (10)$$

Furthermore, $S_c(\kappa/T_b)$ gets the following simpler form: $S_c(\kappa/T_b) = (|C_p(f)|^2 * |C_p(f)|^2)|_{f=\kappa/T_b}$.

Note that white noise and interferences contribute to $S_y^{(\kappa)}$ only when $\kappa = 0$. Otherwise, they are not present.

To substantiate the approximation in (8), Fig. 3 shows $|S_k^l(f)|_{f=\kappa/T_b}$ for a set of maximal length PN codes of length $L_c = 127$ sampled twice per chip and a raised cosine chip waveform with roll-off coefficient $\beta = 0.9$. Fig. 3 also shows $|S_k^l(f)|_{f=\kappa/T_b}$ computed by averaging the output of a RAKE

receiver with 2×127 correlators, which is computationally equivalent to the matched filter—for a nonperiodic code. The parameters for this simulation are the same than for the periodic case: $L_c = 127$ and raised cosine chip waveform with $\beta = 0.9$. The spectral estimation is obtained by averaging over 10 bits.

B. Fingers Location and Beamforming

Let the matrices $S_y^{(\kappa)}$ and $S_y^{(0)}$ be defined as $S_y(\kappa)$ in (9) evaluated at values $\kappa \neq 0$ and $\kappa = 0$, respectively. For $\kappa = 0$, define the “cleaned” version of $S_y^{(0)}$ as $C_y^{(0)} = S_y^{(0)} - \gamma_{\min} \mathbf{I}$, where γ_{\min} is the smallest eigenvalue of $S_y^{(0)}$ ideally equal to σ_n^2 in accordance with (9).

Lemma: The matrix pencil

$$\left\{ S_y^{(\kappa)} - \lambda_i C_y^{(0)} \right\} \mathbf{w}_i = 0 \quad (11)$$

has L_1 nonzero generalized eigenvalues equal to

$$\lambda_i = \frac{S_c \left(\frac{\kappa}{T_b} \right)}{S_c(0)} e^{j2\pi\kappa(\tau_1^i/T_b)} \quad (12)$$

and the corresponding generalized eigenvector satisfies

$$\mathbf{w}_i^H \mathbf{a}(\boldsymbol{\theta}_k^l) \propto \delta_{k1} \delta_{il} \quad (13)$$

i.e., \mathbf{w}_i is orthogonal to each $\mathbf{a}(\boldsymbol{\theta}_k^l)$, $1 \leq k \leq J$ and $1 \leq l \leq L_k$, except $\mathbf{a}(\boldsymbol{\theta}_1^i)$.

Proof: Substituting (9) and (10) into (11) results in

$$\left\{ S_c \left(\frac{\kappa}{T_b} \right) \sum_{l=1}^{L_1} p_1^l \mathbf{a}(\boldsymbol{\theta}_1^l) \mathbf{a}^H(\boldsymbol{\theta}_1^l) e^{j2\pi\kappa(\tau_1^l/T_b)} - \lambda_i S_c(0) \sum_{k=1}^J \sum_{l=1}^{L_k} p_k^l \mathbf{a}(\boldsymbol{\theta}_k^l) \mathbf{a}^H(\boldsymbol{\theta}_k^l) \right\} \mathbf{w}_i = \mathbf{0}. \quad (14)$$

It is obvious that the λ_i values in (12) cancel one term in each of the summations in (14); therefore, they drop the rank of the matrices in the pencil by one unit. Therefore, the λ_i values in (12) are generalized eigenvalues of the pencil in (11). In order to satisfy the equation in (11), the i th generalized eigenvector has to satisfy the relation in (13).

Thus, the time location of the l th finger may be extracted from the l th eigenvalue phase as

$$\hat{\tau}_1^i = \frac{T_b}{2\pi\kappa} \arg(\lambda_i) \quad (15)$$

whereas the corresponding eigenvector provides the beamformer for extracting the i th finger $1 \leq i \leq L_1$.

From (12), it is obvious that $\kappa = 1$ provides the absolute time location of the fingers without indeterminacy within a bit interval. Therefore, if there is no synchronization available, i.e., τ_1^l might take any value in $[0, T_b]$, then $\kappa = 1$ is required; otherwise, there is no unique relation between generalized eigenvalue phase and time delay.

On the other hand, the difference between the phase of two generalized eigenvalues corresponding to two SDC paths with close time delay is proportional to κ . Therefore, the larger the κ , the larger the spread of phases and, therefore, the better resolution (i.e., capability to distinguish from two fingers close in time).

The way to apply the algorithm herein is as follows: If no synchronization information is available, then the algorithm is run once with $\kappa = 1$ to get a rough estimate of the synchronization. After coarse code synchronism acquisition, κ is set to a highest value that assures nonambiguity. This value is $\kappa = \tau_{\max}/T_b$, where τ_{\max} is the maximum delay spread produced by the channel. If synchronization information within an accuracy of α s is available, then κ is set to $\kappa = \alpha/T_b$.

C. Improved Sensitivity in Time Delay Estimation and Multipath Extraction

In the previous subsection, we shown that the phases of the L_1 largest¹ generalized eigenvalues of the matrix pencil $\{\mathbf{S}_y^{(\kappa)} - \lambda_i \mathbf{C}_y^{(0)}\} \mathbf{w}_i = 0$ provide an estimation of the finger locations, whereas the corresponding generalized eigenvectors extract each of the fingers and null out the interferences. Although, ideally, there are only L_1 nonzero generalized

¹Since $\mathbf{S}_y^{(\kappa)}$ is not Hermitian for $\kappa \neq 0$, the generalized eigenvalues of $\{\mathbf{S}_y^{(\kappa)}, \mathbf{C}_y^{(0)}\}$ are complex, and the term "largest" refers to the module.

eigenvalues, the finite number of snapshots used to estimate the $\mathbf{S}_y^{(\kappa)}$ matrices means that they are not exactly rank L_1 , but there are $N - L_1$ small generalized eigenvalues. According to (9), $\mathbf{C}_y^{(0)}$ is rank $L = \sum_{k=1}^J L_k$, which is assumed to be equal or smaller than the number of antenna elements N . If L is smaller than N , $\mathbf{C}_y^{(0)}$ is singular, and the matrix pencil $\{\mathbf{S}_y^{(\kappa)}, \mathbf{C}_y^{(0)}\}$ in (14) is ill conditioned. We propose two ways to circumvent this problem.

First, since the L_1 -rank subspace spanned by the columns of $\mathbf{S}_y^{(\kappa)}$ is contained in the L -rank subspace of $\mathbf{C}_y^{(0)}$, it can be easily shown that the weight vectors \mathbf{w}_i resulting from (14) are also contained in the range space of $\mathbf{C}_y^{(0)}$. Let $\mathbf{\Gamma}_s$ and \mathbf{E}_s be the matrices formed with the nonzero eigenvalues and associated eigenvectors of $\mathbf{C}_y^{(0)}$, respectively. The weight vector can be expressed as $\mathbf{w}_i = \mathbf{E}_s \mathbf{t}_i$, where \mathbf{t}_i is the generalized eigenvector of the matrix pencil in (11) compressed onto the subspace spanned by the \mathbf{E}_s columns

$$\{\mathbf{E}_s^H \mathbf{S}_y^{(\kappa)} \mathbf{E}_s - \lambda_i \mathbf{\Gamma}_s\} \mathbf{t}_i = \mathbf{0}. \quad (16)$$

Thus, λ_i and \mathbf{t}_i can also be computed via the eigendecomposition $\mathbf{\Gamma}_s^{-1} \mathbf{E}_s^H \mathbf{S}_y^{(\kappa)} \mathbf{E}_s \mathbf{t}_i = \lambda_i \mathbf{t}_i$.

The determination of the total number of paths L might prove to be a drawback in a practical application of this method. The SWNR for a CDMA link is usually negative, prior to the signal being passed through the code correlator. The noise power in the $\mathbf{C}_y^{(0)}$ estimation is dictated by this typically negative SWNR. This makes it difficult to obtain an accurate estimate of the number of sources, especially when $\mathbf{C}_y^{(0)}$ is estimated from a few number of samples.

A second way to circumvent the singularity of $\mathbf{C}_y^{(0)}$ is to solve the eigenproblem $\{\mathbf{S}_y^{(\kappa)} - \lambda_i' \mathbf{S}_y^{(0)}\} \mathbf{w}_i' = 0$, which is well conditioned, rather than $\{\mathbf{S}_y^{(\kappa)} - \lambda_i \mathbf{C}_y^{(0)}\} \mathbf{w}_i = 0$.

Proposition: The argument of the generalized eigenvalues λ_i' in $\{\mathbf{S}_y^{(\kappa)} - \lambda_i' \mathbf{S}_y^{(0)}\} \mathbf{w}_i' = 0$ is the same as the phase of λ_i in $\{\mathbf{S}_y^{(\kappa)} - \lambda_i \mathbf{C}_y^{(0)}\} \mathbf{w}_i = 0$.

Proof: See Appendix B.

Proposition: The generalized eigenvector \mathbf{w}_i' of $\{\mathbf{S}_y^{(\kappa)} - \lambda_i' \mathbf{S}_y^{(0)}\} \mathbf{w}_i' = 0$ maximizes the ratio of the i th multipath power to the interference plus noise powers $i = 1, \dots, L_1$. For example, \mathbf{w}_i' corresponds to the minimum variance distortionless response (MVDR) solution $\mathbf{w}_i' = \mathbf{R}_{xx}^{-1} \mathbf{a}(\boldsymbol{\theta}_1^i)$ for the extraction of the $i = 1, \dots, L_1$ SDC paths.

Proof: See Appendix C.

It is well known that the MVDR solution behaves better than the *zero forcing* approach given above in a noisy environment. Moreover, there is no need to estimate the signal subspace of $\mathbf{S}_y^{(0)}$ and its previously mentioned problems. In Section V, we compare the performance of both approaches.

In any case, when the total number of paths (SDC + MUAI's) L is larger than N , both approaches are equivalent.

D. Estimation of SDC Number of Paths

The first approach in the above section first requires the estimation of the total number of incoming paths L . This estimation might be carried out based on the *information criteria* [23]. However, a long time to average $\mathbf{S}_y^{(0)}$ is required to achieve a reliable estimation, especially when the SNR is small.

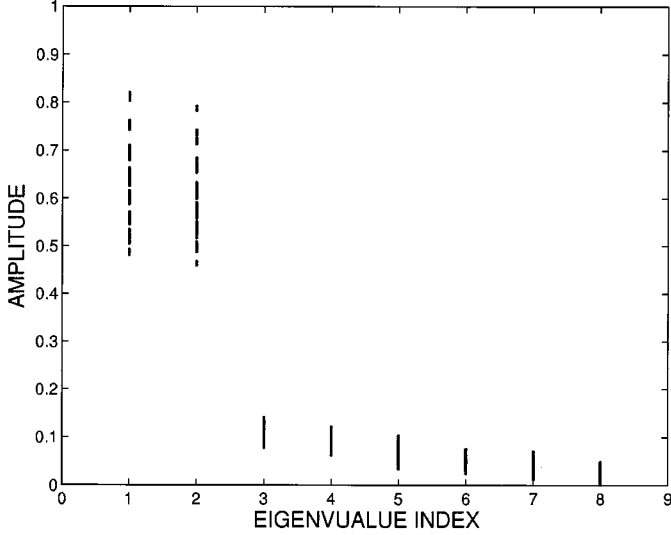


Fig. 4. Amplitude of the generalized eigenvalues of $\{\mathbf{S}_y^{(\kappa)}, \mathbf{S}_y^{(0)}\}$.

The estimation of the number of paths of the desired user and their relative delay is an extremely simple task using the generalized eigendecomposition of $\{\mathbf{S}_y^{(\kappa)}, \mathbf{S}_y^{(0)}\}$. We prove in Sections III-B and III-C that the matrix pencil $\{\mathbf{S}_y^{(\kappa)}, \mathbf{S}_y^{(0)}\}$ has asymptotically only L_1 non-null generalized eigenvalues. Because they are caused by the noise and the finite number of samples involved in the $\mathbf{S}_y^{(\kappa)}$ and $\mathbf{S}_y^{(0)}$ estimation, all the generalized eigenvalues of the above pencil are nonzero. L_1 of them are complex random variables with $(s_c(\kappa/T_b)/s_c(0))e^{j2\pi\kappa(\tau_1^l/T_b)}(\gamma_i/(\gamma_i + \sigma_n^2))$ mean, whereas the rest $N - L_1$ are complex random variable with zero mean. Thus, the statistical distribution of the L_1 generalized eigenvalues module is different from the distribution of the module of the remaining generalized eigenvalues. For a given κ and scenario, i.e., angular path separation and SWNR, the estimated generalized eigenvalues modules are distributed around two clearly different regions. Therefore, the number of SDC paths L_1 is accurately given by the number of generalized eigenvalues whose module passes a threshold. For a given scenario, κ value, and number of averaged samples, the threshold is computed empirically off-line. Simulations have shown that values around 0.4 are good for almost any scenario.

To substantiate the above statement we show the next simulation. Fig. 4 shows a 1024 independent trial Monte Carlo simulation. Each trial computes $\mathbf{S}_y^{(\kappa)}$ and $\mathbf{S}_y^{(0)}$ averaging over a 10-bit period. No *a priori* information of the code synchronism is assumed; therefore, $\kappa = 1$ was used. The scenario consists of three sources (SDC + 2 MUAI's) arriving at a uniform linear antenna array with eight elements. The SDC's arrive through two paths with angles of arrival of 0 and 10°, respectively. The relative delay between both paths is two chips. The SWNR of both paths is 0 and -1.5 dB, respectively. The MUAI's arrive at 30 and -20° with power levels 20 and 22 dB over the strongest path of the SDC, respectively. The chip waveform for the three users is raised cosine with $\beta = 0.5$. Fig. 4 shows that when setting a threshold between 0.2–0.4, the algorithm estimates the SDC number of paths L_1 within an error probability smaller than 1/1024.

1) *Multipaths Arriving with Same Delay:* Two or more multipaths might arrive to the center of the array with such small relative delay that they are 100% coherent for a given sampling rate. In this case, the algorithm herein treats those rays as only one and provides the delay common to all of them. In addition, the algorithm provides the beamformer that maximizes the SINR for the paths arriving with the same delay.

Let $L_s \leq L_1$ paths of the SDC arrive with the same delay. We notate these L_s paths as the last ones $l = L_1 - L_s + 1, \dots, L_1$. Since $\tau_1^{L_1-L_s+1} = \tau_1^{L_1-L_s+2} = \dots = \tau_1^{L_1}$, (2) for the signal model can be reformulated as

$$\mathbf{x}(t) = \sum_{k=1}^J \sigma_k \sum_{l=1}^{L'_k} \rho'_k \mathbf{a}'(\boldsymbol{\theta}'_k) \sum_{n=-\infty}^{\infty} b_k(n) c_k(t - nT_b - \tau_k^l) + \mathbf{n}(t) \quad (17)$$

where L'_k , ρ'_k , and $\mathbf{a}'(\boldsymbol{\theta}'_k)$ remain the same as in (2) for $k \neq 1$, i.e., $L'_k = L_k$, $\rho'_k = \rho_k$, and $\mathbf{a}'(\boldsymbol{\theta}'_k) = \mathbf{a}(\boldsymbol{\theta}_k)$. For $k = 1$, $L'_1 = L_1 - L_s + 1$, and $\rho'_1 = \rho_1$, $\mathbf{a}'(\boldsymbol{\theta}'_1) = \mathbf{a}(\boldsymbol{\theta}_1)$ only for $l = 0, \dots, L_1 - L_s$. When $k = 1$ and $l = L_1 - L_s + 1$, the definitions in (2) become

$$\rho_1^{(L'_1)'} = \rho_1^{(L_1-L_s+1)} \quad (18)$$

$$\mathbf{a}'(\boldsymbol{\theta}'_1^{(L'_1)'}) = \sum_{l=L_1-L_s+1}^{L_1} \frac{\rho_1^l}{\rho_1^{(L_1-L_s+1)}} \mathbf{a}(\boldsymbol{\theta}_1^l). \quad (19)$$

Note that the new array manifolds $\mathbf{a}'(\boldsymbol{\theta}'_k)$ remain unaltered for all the users and rays, except for those rays that are 100% coherent with other multipaths. However, for those multipaths arriving with nondistinguishable delays, we can still write the same signal model as in (2), where the vector $\mathbf{a}(\boldsymbol{\theta}_k)$ is substituted by a linear combination of array manifolds corresponding to those 100% coherent multipaths.

From the notation in (17)–(19) and using the second proposition in Section III-C, it obviously follows that the non-null generalized eigenvectors of the pencil $\{\mathbf{S}_y^{(\kappa)}, \mathbf{S}_y^{(0)}\}$ in a scenario with same-delay are given by

$$\mathbf{w}_l = \mathbf{S}_y^{(0)-1} \mathbf{a}'(\boldsymbol{\theta}'_1) \quad \text{for } l = 1, \dots, L'_1. \quad (20)$$

Note that $\mathbf{S}_y^{(0)-1}$ is the standard space-only covariance matrix. The classical array processing theory—the Wiener optimum filter—proves that the weight vector in (20) provides the maximum SINR where here, the desired signal is understood to comprise all the SDC rays arriving with the same delay.

2) *Multipaths Arriving at Close Angles—Unique Optimum Beamformer:* In [24], the angular spread of the multipath at the base station is known to be not greater than 5°. Moreover, the dimensions of the antenna array are conditioned by economic and environmental factors. Just as an example, an aperture size of ten wavelengths means a 6° beamwidth for the best of the cases, i.e., pointing to the broadside. Under these angular parameters, trying to resolve the L_1 SDC paths leads to undesirable situations, as will be shown next.

The weight vectors \mathbf{w}_l , computed as described above, place deep nulls in the MUAI directions of arrival and in the directions

of the $L_1 - 1$ remaining paths as well. If the separation between 2 SDC rays is smaller than the minimum beamwidth achievable with the given aperture, placing nulls toward the other $L_1 - 1$ SDC paths leads to beams pointing off the desired path direction. This situation is undesirable because the beamformer \mathbf{w}_l loses gain toward θ_1^l in order to place nulls at directions where it is not needed. Note that all the L_1 paths contain the same desired signal. Fig. 5 illustrates this situation. The SDC arrives at angles 0° and 5° . There are two interferences arriving at -20° and 30° . The rest of parameters are not substantial to this explanation. Fig. 5 shows the gain pattern provided by \mathbf{w}_1 and \mathbf{w}_2 when the algorithm herein is applied to a uniform linear array of eight elements separated half a wavelength.

When the electrical environment of the base station and its antenna dimensions suggest multipaths arriving within an angular spread smaller than the minimum beamwidth, we should apply a unique beamformer to the L_1 estimated fingers $\mathbf{w}_1 = \mathbf{w}_2 \cdots = \mathbf{w}_{L_1} = \mathbf{w}$. \mathbf{w} should be still orthogonal to the MUAI's array manifold, i.e.

$$\mathbf{w}^H \mathbf{a}(\theta_k^l) \propto \delta_{k1}. \quad (21)$$

Note that, as opposed to (13), in (21), the orthogonality to the rest of SDC multipaths is not implied.

Let \mathbf{W} be formed by the columns \mathbf{w}_l $l = 1, \dots, L_1$, where \mathbf{w}_l are the non-null generalized eigenvectors of the pencil $\{\mathbf{S}_y^{(\kappa)}, \mathbf{S}_y^{(0)}\}$. Further, let $\boldsymbol{\alpha}$ be a $N \times 1$ vector. Any linear combination of \mathbf{w}_l may be expressed as

$$\mathbf{w} = \mathbf{W}\boldsymbol{\alpha}. \quad (22)$$

Each and every \mathbf{w}_l satisfies (21); therefore, any linear combination of \mathbf{w}_l guaranties the orthogonality to all MUAI steering vectors. Using this orthogonality property plus the i.i.d. characteristic of the noise, we can state that the maximization problem

$$\max_{\boldsymbol{\alpha}} \frac{\boldsymbol{\alpha}^H \mathbf{W}^H \mathbf{S}_y^{(0)} \mathbf{W} \boldsymbol{\alpha}}{\sigma_n^2 \boldsymbol{\alpha}^H \mathbf{W}^H \mathbf{W} \boldsymbol{\alpha}} \quad (23)$$

is equivalent to maximizing the $(S + N)/N$ or the SNR.

It is well known that the $\boldsymbol{\alpha}$ solution to the maximization problem in (23) is given by the "largest" generalized eigenvector of the $L_1 \times L_1$ matrix pencil

$$\{\mathbf{W}^H \mathbf{S}_y^{(0)} \mathbf{W} - \mu \mathbf{W}^H \mathbf{W}\} \boldsymbol{\alpha} = 0. \quad (24)$$

Fig. 6 illustrates the gain pattern provided by $\mathbf{w} = \mathbf{W}\boldsymbol{\alpha}$ under the same scenario as in Fig. 5.

3) *Optimum Combination of the Beamformers Output:* Previous sections described a technique to estimate the L_1 code synchronism delays τ_1^l and weight vectors \mathbf{w}_l that extract the SDC l th path and cancel the interferences. According to this statement, the inner product $\beta_l(n) = \mathbf{w}_l^H \mathbf{y}(nT_b + \tau_1^l)$ follows the expression

$$\begin{aligned} \beta_l(n) &= \mathbf{w}_l^H \mathbf{y}(nT_b + \tau_1^l) \\ &= b_1(n) \sigma_1 \rho_1^l \mathbf{w}_l^H \mathbf{a}(\theta_1^l) + \mathbf{w}_l^H \mathbf{n}_y(nT_b + \tau_1^l) \end{aligned} \quad (25)$$

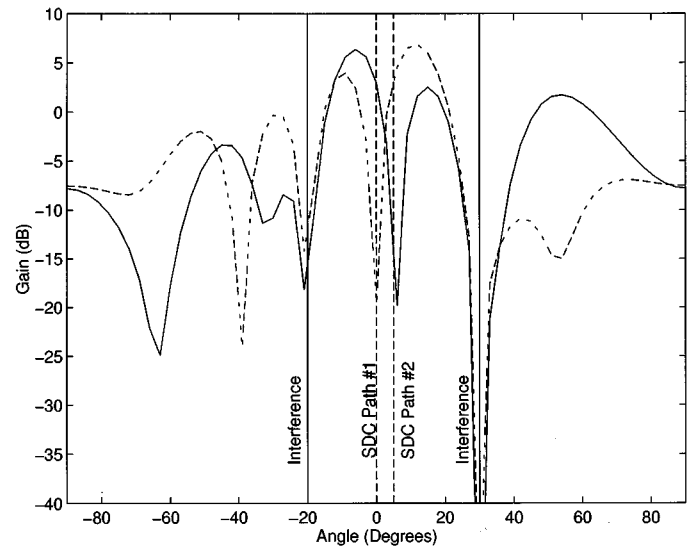


Fig. 5. Gain pattern achieved by \mathbf{w}_l $l = 1, 2$.

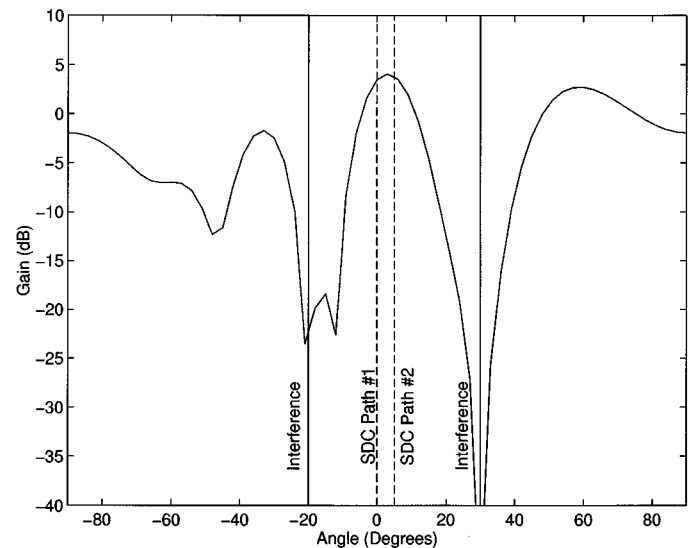


Fig. 6. Gain pattern achieved by \mathbf{w} .

where we have used the signal model in (4) and assumed that the codes $c_k(t)$ are normalized to have power equal to 1.

Even in the case where the weight vector \mathbf{w}_l is not orthogonal to the $L_1 - 1$ remaining fingers, (25) still holds by just changing $\sigma_1 \rho_1^l \mathbf{w}_l^H \mathbf{a}(\theta_1^l)$ for the proper combination of the L_1 SDC path contributions.

The next and last step in this time-space filtering technique for CDMA consists of the optimum combination of the L_1 beamspace-time samples $\beta_l(n)$ to maximize the SINR. Let $\boldsymbol{\beta}(n)$ and $\mathbf{n}_w(n)$ be the $L_1 \times 1$ vectors formed with the entries $\beta_l(n)$ and $\mathbf{w}_l^H \mathbf{n}_y(nT_b + \tau_1^l)$, $l = 1, \dots, L_1$, respectively. Now, the objective is to find the $L_1 \times 1$ vector $\boldsymbol{\gamma}$ such that $\hat{\mathbf{b}}(n) = \boldsymbol{\gamma}^H \boldsymbol{\beta}(n)$ maximizes the SINR.

The beamspace-time vector $\boldsymbol{\beta}(n)$ is formed with the outputs of the weight vectors \mathbf{w}_l , which were proven to be orthogonal to all the interferences. Therefore, there is no interference contribution to the vector $\boldsymbol{\beta}(n)$, as shown in (25). Under these conditions, the SINR is maximized by maximizing

the SNR. Moreover, such maximization may be achieved by maximizing the output power $E[b(n)b^*(n)]$ constrained to γ , exhibiting unitary gain for the noise vector $\mathbf{n}_w(n)$. $\mathbf{n}_w(n)$ is the beamspace-time vector formed with the noise components of the outputs of the weight vectors, i.e., the l th entry of $\mathbf{n}_w(n)$ is $\mathbf{n}_w^l(n) = \mathbf{w}_l^H \mathbf{n}_y(nT_b + \tau_1^l)$. In other words, the maximization of the SINR can be expressed as

$$\max_{\boldsymbol{\gamma}} E[\boldsymbol{\gamma}^H \boldsymbol{\beta}(n) \boldsymbol{\beta}^H(n) \boldsymbol{\gamma}] \quad (26)$$

$$\text{constrained to: } E[\boldsymbol{\gamma}^H \mathbf{n}_w(n) \mathbf{n}_w^H(n) \boldsymbol{\gamma}] = 1. \quad (27)$$

$E[\mathbf{n}_w(n) \mathbf{n}_w^H(n)] = \mathbf{I}$ because the entries of $\mathbf{n}_w(n)$ are samples of noise taken at different snapshots; therefore, the constraint in (27) becomes

$$\boldsymbol{\gamma}^H \boldsymbol{\gamma} = 1. \quad (28)$$

The value of $\boldsymbol{\gamma}$ that satisfies the maximization problem in (26) and (28) is the eigenvector corresponding to the largest eigenvalue of the matrix

$$\mathbf{R}_{\boldsymbol{\beta}} = E[\boldsymbol{\beta}(n) \boldsymbol{\beta}^H(n)]. \quad (29)$$

Thus, the weight vector $\boldsymbol{\gamma}$ that coherently adds up the outputs of the w_l beamformers sampled at τ_1^l is computed as the *largest* eigenvector of $\mathbf{R}_{\boldsymbol{\beta}}$ in (29). $\mathbf{R}_{\boldsymbol{\beta}}$ can be computed by averaging $\boldsymbol{\beta}(n) \boldsymbol{\beta}^H(n)$ over $n = 1, \dots, N_b$, where N_b is the number of bits we can assume for the channel response to be constant.

IV. 2-D RAKE RECEIVER

A matched filter based on the SDC code waveform $h(n) = c_1^*(-n)$ computes $S_c L_c$ output samples per bit, where S_c is the number of samples per chip, and L_c is the number of chips per bit. Each output sample implies $S_c L_c$ complex multiplications and $S_c L_c - 1$ sums. This amount of computations is not suitable for real-time processing for cellular communications and the present technology. However, most of the CDMA receivers incorporate a RAKE structure, as depicted in Fig. 1. The computational cost of a RAKE receiver with T taps is $S_c L_c / T$ times smaller than the matched filter. Moreover, the RAKE receiver performs a parallel implementation of it. The trade-off for the computational cost reduction is the need for coarse code synchronism, i.e., the fingers must lie into the time spanned by the T RAKE taps.

Up to this point, the algorithms have been described in conjunction with hardware based on the matched filter. However, they do not strictly require samples all along the bit duration. The instrumental property the algorithm exploits is the difference between the spectrum of squared waveform components from the SDC—fingers—and the MUAI's. Therefore, the algorithm still works when only part of the matched filter output samples are available as long as the samples span the period of time when the fingers occur. Now, the number of samples to process per bit is T from each of the N antennas.

When the algorithm presented herein is applied in conjunction with a 2-D-RAKE receiver with T taps, the time-varying

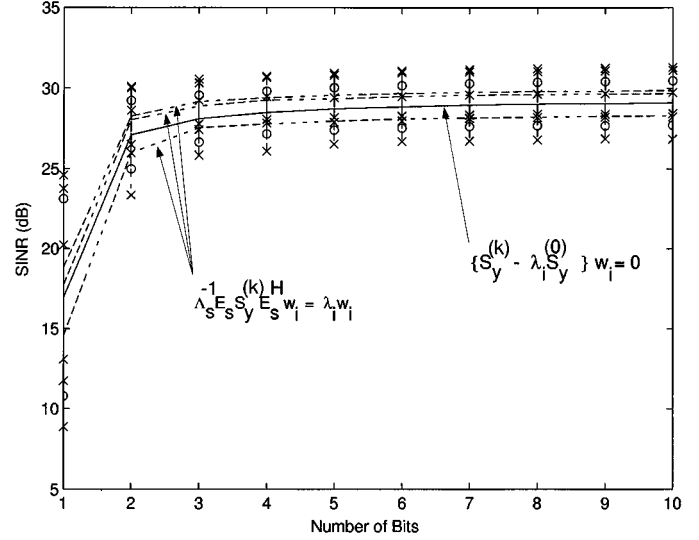


Fig. 7. SINR convergence when solving $\Gamma_s^{-1} \mathbf{E}_s^H \mathbf{S}_y^{(s)} \mathbf{E}_s \mathbf{t}_i = \lambda_i \mathbf{t}_i$ or $\{\mathbf{S}_y^{(s)}, \mathbf{S}_y^{(0)}\}$.

covariance matrix $\mathbf{R}_y(t)$ can be computed only inside a rectangular window of length $T(T_c/S_c)$. Equation (5) becomes $\mathbf{R}_y(t) = E[\mathbf{y}(t) \mathbf{y}^H(t) \text{rect}(tS_c/TT_c)]$, and its sampled version is given by

$$\mathbf{R}_y(n) = E \left[\mathbf{y}(n) \mathbf{y}^H(n) \text{rect} \left(\frac{n}{T} \right) \right]. \quad (30)$$

A DFT of T samples collected at a sampling rate of S_c/T_c provides spectral lines at frequencies

$$f = n \frac{S_c}{TT_c} = n \frac{L_c S_c}{T} \frac{1}{T_b}. \quad (31)$$

The smallest spectral line provided by the DFT $n = 1$ is $(L_c S_c / T)(1/T_b)$, which corresponds to a value of

$$\kappa = \frac{L_c S_c}{T}. \quad (32)$$

The value of κ in (32) is obviously larger than 1. However, the ambiguity in the finger time location for the value of κ in (32) is $\pm T(T_c/S_c)$, which is exactly the time span of the RAKE receiver. Therefore, there is no such ambiguity.

A summary of the algorithm is presented in Section VI. Simulations illustrating the performances are shown in Section V.

V. SIMULATIONS

Extensive simulations of both the matched filter based and the 2-D-RAKE receiver algorithms were performed. Regarding the algorithm working in conjunction with N matched filters, Fig. 7 compares the convergence rate of both approaches in Section III-C. The simulated scenario consists of three users. The SDC arrives via two paths at 0° and 10° , respectively, with a one chip delay between them. The SWNR for the direct path is -5 dB (prior to the matched filter). The amplitude of the second

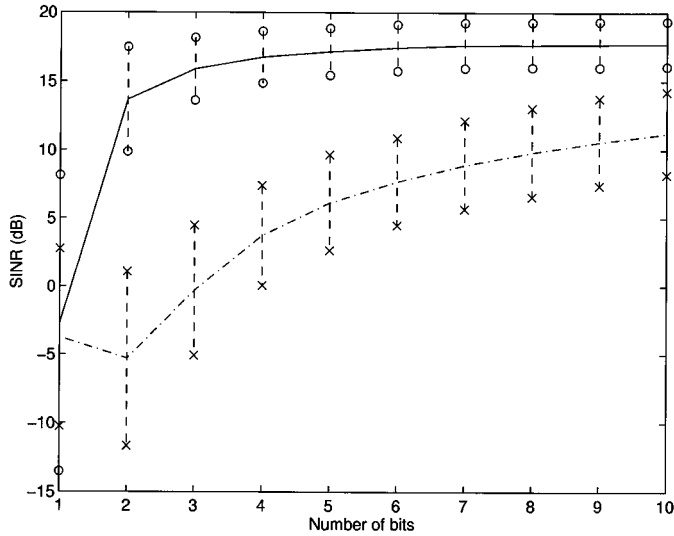


Fig. 8. 2-D RAKE receiver. SINR convergence.

ray is 1.5 dB below the direct path. The interferences arrive at 30° and -20° with respective powers 20 and 22 dB above the direct path of the SDC. The chip waveform is a raised cosine with $\beta = 0.5$. Fig. 7 was obtained by a Monte Carlo simulation with 1024 independent trials. When using the subspace compression approach—dashed lines—simulations were run for a correct estimation of the number of paths, which is an overestimation by one path and an underestimation by one path. Fig. 7 shows that subspace compression leads to a better performance when the total number of paths is estimated correctly. Overestimation of L degrades the SINR less than underestimation. The second of the above approaches gets a better performance than the subspace compression when the total number of paths in this first approach is underestimated by only one path. Bigger errors in the number of paths lead to even worse SINR. Besides the problem of computing accurately the number of paths, computing the generalized eigenvalues of $\{\mathbf{S}_y^{(\kappa)}, \mathbf{S}_y^{(0)}\}$ requires less computation load. Both approaches use a value of $\kappa = 12$. A common beamformer for the two paths was used since the multipaths angular spread is smaller than the minimum beamwidth achievable with the given array.

Regarding the 2-D-RAKE receiver structure, only simulations incorporating the $\{\mathbf{S}_y^{(\kappa)}, \mathbf{S}_y^{(0)}\}$ eigendecomposition approach are presented. The 2-D-RAKE receiver comes out from clearly practical implementation viewpoint, and thus, a slight decrement of performances is sacrificed to keep the algorithm as robust and simple as possible.

Fig. 8 shows a Monte Carlo simulation with 1024 independent trials for the 2-D-RAKE receiver. Three users arrive to a uniform linear array with eight elements separated by a half wavelength. The SDC arrives via two paths at 0° and 5° , respectively. The relative delay between paths is one chip. The SWNR for the direct path is -15 dB (prior to the matched filter). The amplitude of the second ray is 1.5 dB below the direct path. The interferences arrive at 30° and -20° with respective powers of 20 and 22 dB above the direct path of the SDC. The chip waveform is a raised-cosine with $\beta = 0.5$. The solid line in Fig. 8 corresponds to the algorithm proposed herein, whereas dashed

line corresponds to the 2-D RAKE receiver proposed by Wong *et al.* [12]. It can be seen that SINR mean value converges faster, and the variance is smaller when using the algorithm proposed herein.

VI. CONCLUSION

A technique for antenna array CDMA receivers that provides the optimum combination of space-time samples for maximizing the SINR for the *signal with the desired code* (SDC) by canceling strong *multiuser access interference* (MUAI) and optimally combining the multipath has been proposed.

Table I summarizes the 2-D-RAKE receiver algorithm.

APPENDIX A $\mathbf{S}_y(f)$ ANALYSIS

Proposition:

$$\mathbf{S}_y(f) = \sum_{k=1}^J \sum_{l=1}^{L_k} p_k^l \mathbf{a}(\boldsymbol{\theta}_k^l) \mathbf{a}^H(\boldsymbol{\theta}_k^l) S_k^l(f) + \sigma_n^2 \mathbf{I} \delta(f) \quad (33)$$

where

$$S_k^l(f) = \begin{cases} S_c(0) \delta(f), & \text{if } k \neq 1 \\ e^{j2\pi\tau_k^l f} S_c(f), & \text{if } k = 1 \end{cases} \quad (34)$$

and $p_k^l = \sigma_k^2 |\rho_k^l|^2 \sigma_b^2$, $S_c(f) = [(|C_p(f)|^2 * |C_p(f)|^2) T(f)] * \text{sinc}(fT_b)$

$$T(f) = \sum_{n=-\infty}^{\infty} e^{j2\pi f n T_b} = \sum_{n=-\infty}^{\infty} \delta\left(f - \frac{n}{T_b}\right) \quad (35)$$

and $C_p(f)$ is the Fourier transform of the chip pulse waveform.

Proof: From the definition of \mathbf{S}_y in (5) and (6) and using the expression for the continuous time Fourier transform, the \mathbf{S}_y definition may be rewritten as

$$\mathbf{S}_y(f) = \int_{-\infty}^{\infty} E \left[\mathbf{y}(t) \mathbf{y}(t)^H \text{rect}\left(\frac{t}{T_b}\right) \right] e^{j2\pi f t} dt. \quad (36)$$

Substituting the signal model assumed for $\mathbf{y}(t)$ given in (4) into (36) results in

$$\begin{aligned} \mathbf{S}_y(f) = \int_{-\infty}^{\infty} E \left[\left\{ \sum_{k=1}^J \sigma_k \sum_{l=1}^{L_k} \rho_k^l \mathbf{a}(\boldsymbol{\theta}_k^l) \sum_{n=-\infty}^{\infty} \right. \right. \\ \left. \left. \cdot b_k(n) c_k(t - nT_b - \tau_k^l) * c_1(-t) + \mathbf{n}_y(t) \right\} \right. \\ \left. \left\{ \sum_{p=1}^J \sigma_p \sum_{q=1}^{L_p} \rho_p^q \mathbf{a}(\boldsymbol{\theta}_p^q) \sum_{m=-\infty}^{\infty} b_p(m) c_p(t - mT_b - \tau_p^q) \right. \right. \\ \left. \left. * c_1(-t) + \mathbf{n}_y(t) \right\}^H \text{rect}\left(\frac{t}{T_b}\right) \right] e^{-j2\pi f t} dt. \quad (37) \end{aligned}$$

We assume that user signals and noise are uncorrelated and that bit values from two different users are also uncorrelated. In addition, we assume that the bits sent by a given user at different times are uncorrelated. Thus, $E[b_k(n)b_p(m)] = \delta_{kp}\delta_{nm}$. With these assumptions (37) simplifies to

$$\begin{aligned} \mathbf{S}_y(f) = & \sigma_b^2 \int_{-\infty}^{\infty} \left(\sum_{k=1}^J \sigma_k^2 \sum_{l=1}^{L_k} \sum_{q=1}^{L_k} \rho_k^l \rho_k^{q*} \mathbf{a}(\boldsymbol{\theta}_k^l) \mathbf{a}^H(\boldsymbol{\theta}_k^q) \right. \\ & \sum_{n=-\infty}^{\infty} \{c_k(t - nT_b - \tau_k^l) * c_1(-t)\} \\ & \{c_k(t - nT_b - \tau_k^q) * c_1(-t)\}^* \\ & \left. + E \left[\mathbf{n}_y(t) \mathbf{n}_y^H(t) \right] \right) \text{rect} \left(\frac{t}{T_b} \right) e^{-j2\pi t f} dt \quad (38) \end{aligned}$$

where we have used the linearity of the operator $E[\cdot]$, i.e., we have interchanged the order of sum, integral, and expected value operators. Now, interchanging the order of integral and sum operators again results in

$$\begin{aligned} \mathbf{S}_y(f) = & \sigma_b^2 \sum_{k=1}^J \sigma_k^2 \sum_{l=1}^{L_k} \sum_{q=1}^{L_k} \rho_k^l \rho_k^{q*} \mathbf{a}(\boldsymbol{\theta}_k^l) \mathbf{a}^H(\boldsymbol{\theta}_k^q) S_k^{lq}(f) \\ & + \int_{-\infty}^{\infty} E \left[\mathbf{n}_y(t) \mathbf{n}_y^H(t) \right] \text{rect} \left(\frac{t}{T_b} \right) e^{-j2\pi t f} dt \quad (39) \end{aligned}$$

where

$$\begin{aligned} S_k^{lq}(f) = & \int_{-\infty}^{\infty} \sum_{n=-\infty}^{\infty} \{c_k(t - nT_b - \tau_k^l) * c_1(-t)\} \\ & \{c_k(t - nT_b - \tau_k^q) * c_1(-t)\}^* \text{rect} \left(\frac{t}{T_b} \right) e^{-j2\pi t f} dt. \quad (40) \end{aligned}$$

We consider stationary and white noise with a variance of σ_n^2 equal at all the antennae. Noise components at two antennae are uncorrelated. Under these assumptions, $\mathbf{S}_y(f)$ in (39) is given by

$$\begin{aligned} \mathbf{S}_y(f) = & \sigma_b^2 \sum_{k=1}^J \sigma_k^2 \sum_{l=1}^{L_k} \sum_{q=1}^{L_k} \rho_k^l \rho_k^{q*} \mathbf{a}(\boldsymbol{\theta}_k^l) \mathbf{a}^H(\boldsymbol{\theta}_k^q) S_k^{lq}(f) \\ & + \sigma_n^2 \mathbf{I} \text{sinc}(fT_b). \quad (41) \end{aligned}$$

At this point, if we prove that

$$S_k^{lq}(f) = \begin{cases} S_c(0)\delta(f), & \text{if } k \neq 1 \\ \delta_{lq} e^{j2\pi\tau_1^l} S_c(f), & \text{if } k = 1 \end{cases} \quad (42)$$

then (33) and (34) are proven as well.

Assuming $c_k(t)$ is real-valued and using elemental FT properties, (40) can be expressed as

$$\begin{aligned} S_k^{lq}(f) = & \sum_{n=-\infty}^{\infty} \left(C_k(f) C_1^*(f) e^{j2\pi f n T_b} e^{j2\pi f \tau_k^l} \right) \\ & * \left(C_k(f) C_1^*(f) e^{j2\pi f n T_b} e^{j2\pi f \tau_k^q} \right) * \text{sinc}(fT_b) \quad (43) \end{aligned}$$

where $C_k(f)$ is the Fourier Transform of the code $c_k(t)$. Note that by construction, PN codes satisfy i) $|C_k(f)| = |C_p(f)|$,

where $C_p(f)$ is the FT of the chip waveform; and ii) the phase of $C_k(f)$ is a white random process with a p.d.f. uniformly distributed in $[0, 2\pi]$.

Let us analyze the cases $k = 1$ and $k \neq 1$.

a) $k = 1$: Using basic algebra manipulations and the convolution definition, we get

$$\begin{aligned} S_1^{lq}(f) = & \sum_{n=-\infty}^{\infty} \left(C_1(f) C_1^*(f) e^{j2\pi f n T_b} e^{j2\pi f \tau_1^l} \right) \\ & * \left(C_1(f) C_1^*(f) e^{j2\pi f n T_b} e^{j2\pi f \tau_1^q} \right) * \text{sinc}(fT_b) \\ = & \sum_{n=-\infty}^{\infty} \left(|C_p(f)|^2 e^{j2\pi f n T_b} e^{j2\pi f \tau_1^l} \right) \\ & * \left(|C_p(f)|^2 e^{j2\pi f n T_b} e^{j2\pi f \tau_1^q} \right) * \text{sinc}(fT_b) \\ = & e^{j2\pi f \tau_1^q} \left(\int_{-\infty}^{\infty} |C_p(s)|^2 |C_p(f-s)|^2 e^{j2\pi s(\tau_1^l - \tau_1^q)} ds \right. \\ & \left. * \sum_{n=-\infty}^{\infty} e^{j2\pi f n T_b} \right) * \text{sinc}(fT_b). \quad (44) \end{aligned}$$

Now, from (44), it is obvious that if $l = q$, then

$$S_1^{lq}(f) = e^{j2\pi f \tau_1^l} \left[(|C_p(f)|^2 * |C_p(f)|^2) T(f) \right] * \text{sinc}(fT_b) \quad (45)$$

where $T(f) = \sum_{n=-\infty}^{\infty} e^{j2\pi f n T_b} = \sum_{n=-\infty}^{\infty} \delta(f - (n/T_b))$.

Otherwise, if $l \neq q$, the integral $\int_{-\infty}^{\infty} |C_p(s)|^2 |C_p(f-s)|^2 e^{j2\pi s(\tau_1^l - \tau_1^q)} ds$ in (44) takes almost negligible values whenever $\tau_1^l - \tau_1^q \geq T_c$, where T_c is the chip length. In particular, for rectangular waveform chips and $\tau_1^l - \tau_1^q = T_c$, the integral value is exactly 0; for other relative delays and chip waveform (as raised cosine), the simulations confirmed the above statement.

The case $\tau_1^l - \tau_1^q < T_c$ is addressed in Section III-D1. In this case, the best way to go is not to distinguish the paths but to find the beamformer that maximizes the SDC power at that instant (chip length).

b) $k \neq 1$: MUAI's belonging to the same system have the same chip pulse shape and $C_k(f) = |C_p(f)| e^{j r_k(f)}$, where $r_k(f)$ is a white random process uniformly distributed in $[0, 2\pi]$. In addition, the PN codes are such that the phases of any two of them are independent. Using the properties in (43) results in

$$\begin{aligned} S_k^{lq}(f) = & \sum_{n=-\infty}^{\infty} \left(|C_p(f)|^2 e^{j(r_k(f) - r_1(f))} e^{j2\pi f n T_b} e^{j2\pi f \tau_k^l} \right) \\ & * \left(|C_p(f)|^2 e^{j(r_k(f) - r_1(f))} e^{j2\pi f n T_b} e^{j2\pi f \tau_k^q} \right) \\ & * \text{sinc}(fT_b). \quad (46) \end{aligned}$$

$e^{j r_k(f)}$ and $e^{j r_1(f)}$ are complex independent random variables with the phase uniformly distributed in $[0, 2\pi]$ and constant modulus; therefore, $e^{j(r_k(f) - r_1(f))} = e^{j r'_k(f)}$ is also a

TABLE I
2-D-RAKE RECEIVER SUMMARY

- Form T vectors ($N \times 1$) $\mathbf{y}^{(n)}(l)$ per bit by stacking the N RAKE receiver outputs at the l -th tap. $l = 1, \dots, T$. n is the bit index.
- Given samples along N_b bits, compute T time-varying correlation matrices as

$$\mathbf{R}_y(l) = \frac{1}{N_b} \sum_{n=1}^{N_b} \mathbf{y}^{(n)}(l) \mathbf{y}^{(n)H}(l)$$

- Compute the Matrices $\mathbf{S}_y^{(0)}$ and $\mathbf{S}_y^{(\kappa)}$ as

$$\mathbf{S}_y^{(0)} = \sum_{l=1}^T \mathbf{R}_y(l), \text{ and}$$

$$\mathbf{S}_y^{(\kappa)} = \sum_{l=1}^T \mathbf{R}_y(l) e^{j2\pi \frac{l}{T} \kappa}$$

- Find the generalized eigenvalues λ_i and eigenvectors \mathbf{w}_i of the matrix pencil

$$\{\mathbf{S}_y^{(k)} - \lambda_i \mathbf{S}_y^{(0)}\} \mathbf{w}_i = 0$$

- Estimate the number of distinguishable SDC paths, L_1 , as the number of generalized eigenvalues whose module is larger than an a priori computed threshold. A threshold equal to 0.45 is a good starting point for most of the scenarios.
- The locations of the multipaths inside the T taps are given by the index

$$\hat{\tau}_1^i = \lfloor \frac{T}{2\pi} \arg(\lambda_i) \rfloor$$

where $\lfloor \cdot \rfloor$ stands for the nearest integer number.

- If the electrical environment allows a SDC multipath angular spread > 3 -dB antenna beamwidth; < 3 -dB antenna beamwidth;
Compute $\beta_i(n) = \mathbf{w}_i^H \mathbf{y}^{(n)}(\hat{\tau}_1^i)$ Form $\mathbf{W} = [\mathbf{w}_1 \dots \mathbf{w}_{L_1}]$
for $i = 1, \dots, L_1$ Compute α as the "largest" gen. eigenvector
of matrix pencil $\{\mathbf{W}^H \mathbf{S}_y^{(0)} \mathbf{W}, \mathbf{W}^H \mathbf{W}\}$
Compute $\beta_i(n) = \alpha^H \mathbf{W}^H \mathbf{y}^{(n)}(\hat{\tau}_1^i)$
for $i = 1, \dots, L_1$
- Form the $L_1 \times 1$ vectors $\beta(n)$ from $\beta_i(n)$ and compute the matrix

$$\mathbf{R}_\beta = \frac{1}{N_b} \sum_{n=1}^{N_b} \beta(n) \beta^H(n)$$

- Compute the \mathbf{R}_β largest eigenvector, γ . The n bit value estimation is given by

$$b(n) = \gamma^H \beta(n)$$

complex independent random variable with the phase uniformly distributed in $[0, 2\pi]$, and therefore

$$S_k^{lq}(f) = \sum_{n=-\infty}^{\infty} e^{j2\pi f n T_b} \left(\int_{-\infty}^{\infty} |C_p(s)|^2 |C_p(f-s)|^2 \cdot e^{j r'_k(s)} e^{j r'_k(f-s)} e^{j 2\pi s \tau_k^l} e^{j 2\pi (f-s) \tau_k^q} ds \right) * \text{sinc}(f T_b). \quad (47)$$

Only if $f = 0$ and $l = q$, the integral in (47) takes a nonzero value, and it simplifies to

$$S_k^{lq}(0) = \int_{-\infty}^{\infty} |C_p(s)|^4 ds = S_c(0). \quad (48)$$

Otherwise, the integral in (47) is zero, and $S_k^{lq}(f) = 0$. This statement holds since $r'_k(s)$ is white, and therefore, $r'_k(s)$ and $r'_k(f-s)$ are uncorrelated for any $f \neq 0$.

At this point, (42) has been proven, and therefore (33) and (34) are proven as well.

APPENDIX B

GENERALIZED EIGENVALUES OF THE PENCIL $\{\mathbf{S}_y^{(\kappa)}, \mathbf{S}_y^{(0)}\}$

Proposition: The argument of the generalized eigenvalues λ'_i in $\{\mathbf{S}_y^{(\kappa)} - \lambda'_i \mathbf{S}_y^{(0)}\} \mathbf{w}'_i = 0$ is the same as the phase of λ_i in $\{\mathbf{S}_y^{(\kappa)} - \lambda_i \mathbf{C}_y^{(0)}\} \mathbf{w}_i = 0$.

Proof: Let us consider the generalized eigendecompositions

$$\{\mathbf{S}_y^{(\kappa)} - \lambda'_i \mathbf{S}_y^{(0)}\} \mathbf{w}'_i = 0 \quad (49)$$

$$\{\mathbf{S}_y^{(\kappa)} - \lambda_i \mathbf{C}_y^{(0)}\} \mathbf{w}_i = 0. \quad (50)$$

The generalized eigenvalues in both problems satisfy the equations

$$|\mathbf{S}_y^{(0)-1} \mathbf{S}_y^{(\kappa)} - \lambda'_i \mathbf{I}| = 0 \quad (51)$$

and

$$|\mathbf{C}_y^{(0)-\dagger} \mathbf{S}_y^{(\kappa)} - \lambda_i \mathbf{I}| = 0 \quad (52)$$

where $(\cdot)^\dagger$ represents pseudo-inverse. Using the eigendecomposition of $\mathbf{C}_y^{(0)}$, (51) and (52) can be rewritten as

$$|[\mathbf{E}_s; \mathbf{E}_n] \mathbf{\Gamma}_{S+I}^{-1} [\mathbf{E}_s; \mathbf{E}_n]^H \mathbf{S}_y^{(\kappa)} - \lambda'_i \mathbf{I}| = 0 \quad (53)$$

and

$$|\mathbf{E}_s \mathbf{\Gamma}_s^{-1} \mathbf{E}_s^H \mathbf{S}_y^{(\kappa)} - \lambda_i \mathbf{I}| = 0 \quad (54)$$

where

$$\mathbf{\Gamma}_{S+I} = \begin{pmatrix} \mathbf{\Gamma}_s + \gamma_{\min} \mathbf{I} & \mathbf{O} \\ \mathbf{O} & \gamma_{\min} \mathbf{I} \end{pmatrix} \quad (55)$$

and \mathbf{E}_n is composed of the eigenvectors of $\mathbf{S}_y^{(0)}$ associated with the $N - L$ smallest eigenvalues.

Now, $\mathbf{S}_y^{(\kappa)}$ spans an L_1 -dimension subspace contained in the L dimension subspace of $\mathbf{C}_y^{(0)}$. Thus, $\mathbf{S}_y^{(\kappa)}$ can be expressed as $\mathbf{S}_y^{(\kappa)} = \mathbf{E}_s \mathbf{\Phi} \mathbf{\Delta}_k \mathbf{\Phi}^H \mathbf{E}_s^H$, where $\mathbf{\Delta}_k$ is an $L_1 \times L_1$ diagonal matrix, and $\mathbf{\Phi}$ is an $L \times L_1$ matrix such that $\mathbf{A}_1 = \mathbf{E}_s \mathbf{\Phi}$, and $\mathbf{A}_1 = [\mathbf{a}(\boldsymbol{\theta}_1^1), \dots, \mathbf{a}(\boldsymbol{\theta}_1^{L_1})]$. Note that the L_1 elements of $\mathbf{\Delta}_k$ are complex-valued since $\mathbf{S}_y^{(\kappa)}$ is not Hermitian. Exploiting $\mathbf{E}_s^H \mathbf{E}_s = \mathbf{I}_L$ and $\mathbf{E}_s^H \mathbf{E}_n = \mathbf{O}$, (53) and (54) are

$$|\mathbf{E}_s (\mathbf{\Gamma}_s + \gamma_{\min} \mathbf{I})^{-1} \mathbf{\Phi} \mathbf{\Delta}_k \mathbf{\Phi}^H \mathbf{E}_s^H - \lambda'_i \mathbf{I}| = 0 \quad (56)$$

and

$$|\mathbf{E}_s \mathbf{\Gamma}_s^{-1} \mathbf{\Phi} \mathbf{\Delta}_k \mathbf{\Phi}^H \mathbf{E}_s^H - \lambda_i \mathbf{I}| = 0. \quad (57)$$

Compressing the matrix pencils inside the determinants onto the subspace spanned by the columns of \mathbf{E}_s , the nonzero eigenvalues for either (13) or (14) may be computed via

$$|\mathbf{\Phi} \mathbf{\Delta}_k \mathbf{\Phi}^H - \lambda'_i (\mathbf{\Gamma}_s + \gamma_{\min} \mathbf{I})| = 0 \quad (58)$$

and

$$|\mathbf{\Phi} \mathbf{\Delta}_k \mathbf{\Phi}^H - \lambda_i \mathbf{\Gamma}_s| = 0 \quad (59)$$

where we have used $|\mathbf{AB}| = |\mathbf{A}| |\mathbf{B}|$. From (58) and (59), it is clear that

$$\lambda'_i = \lambda_i \frac{\gamma_i}{\gamma_i + \gamma_{\min}} \quad (60)$$

where γ_i are the entries of the diagonal of $\mathbf{\Gamma}_s$. γ_i and γ_{\min} are eigenvalues of a Hermitian matrix and are thus real valued. It follows then that the λ'_i phase is the same as that of λ_i , $i = 1, \dots, L_1$.

APPENDIX C

GENERALIZED EIGENVECTORS OF THE PENCIL $\{\mathbf{S}_y^{(\kappa)}, \mathbf{S}_y^{(0)}\}$

Proposition: The generalized eigenvector \mathbf{w}'_i of $\{\mathbf{S}_y^{(\kappa)} - \lambda'_i \mathbf{S}_y^{(0)}\} \mathbf{w}'_i = 0$ maximizes the ratio of the i th multipath power to the interference plus noise powers $i = 1, \dots, L_1$. For example, \mathbf{w}'_i is the MVDR solution $\mathbf{w}'_i = \mathbf{R}_{xx}^{-1} \mathbf{a}(\boldsymbol{\theta}_1^i)$ for the extraction of the $i = 1, \dots, L_1$ SDC paths.

Proof: Note that the matrix $\mathbf{S}_y^{(0)}$ is the conventional spatial correlation matrix typically denoted \mathbf{R}_{xx} . In addition, it is known that the MVDR beamformer places nulls to all the array manifolds of incoming signals except for the desired one, as long as the noise power is small relative to the interferences received power. When the noise and interferences power are comparable, the MVDR beamformer places “shallower nulls” toward the interferences that are deep enough to keep their output level below the noise. Under these considerations, we can state that

$$\mathbf{a}^H(\boldsymbol{\theta}_k^l) \mathbf{S}_y^{(0)-1} \mathbf{a}(\boldsymbol{\theta}_n^m) \approx \delta_{kn} \delta_{lm}. \quad (61)$$

The generalized eigenvectors \mathbf{w}'_i of the matrix pencil $\{\mathbf{S}_y^{(\kappa)}, \mathbf{S}_y^{(0)}\}$ also result in eigenvectors of the matrix $\mathbf{S}_y^{(0)-1} \mathbf{S}_y^{(\kappa)}$. The presence of noise guaranties that $\mathbf{S}_y^{(0)}$ is full rank. Using (9), we get that the eigenvectors \mathbf{w}'_i satisfy

$$\left\{ \mathbf{S}_y^{(0)-1} \sum_{l=1}^{L_1} \mathbf{a}(\boldsymbol{\theta}_1^l) \mathbf{a}^H(\boldsymbol{\theta}_1^l) p_1^l S_1^l \left(\frac{\kappa}{T_b} \right) \right\} \mathbf{w}'_i = \lambda'_i \mathbf{w}'_i. \quad (62)$$

Premultiplying both sides of (62) by $\mathbf{a}^H(\boldsymbol{\theta}_1^i)$ and assuming (61) holds with the equal sign, we get

$$p_1^i S_1^i \left(\frac{\kappa}{T_b} \right) \mathbf{a}^H(\boldsymbol{\theta}_1^i) \mathbf{S}_y^{(0)-1} \mathbf{a}(\boldsymbol{\theta}_1^i) \mathbf{a}^H(\boldsymbol{\theta}_1^i) \mathbf{w}'_i = \lambda'_i \mathbf{a}^H(\boldsymbol{\theta}_1^i) \mathbf{w}'_i \quad (63)$$

where $\mathbf{w}'_i = \mathbf{S}_y^{(0)-1} \mathbf{a}(\boldsymbol{\theta}_1^i)$ is the nontrivial solution in (63) and is therefore the solution to the generalized eigenproblem.

REFERENCES

- [1] J. C. Liberti and T. S. Rappaport, “Analytical results for capacity improvements in CDMA,” *IEEE Trans. Veh. Technol.*, vol. 43, pp. 680–690, Aug. 1994.

- [2] A. Naguib, A. Paulraj, and T. Kailath, "Capacity improvement with base-station antenna array in cellular CDMA," *IEEE Trans. Veh. Technol.*, vol. 43, pp. 691–698, Aug. 1994.
- [3] A. J. Viterbi, *CDMA—Principles of Spread Spectrum Communication*. Reading, MA: Addison-Wesley, 1995.
- [4] B. Suard, A. Naguib, G. Xu, and T. Kailath, "Performance analysis of CDMA mobile communication systems using antenna arrays," in *Proc. ICASSP*, vol. VI, Apr. 1993, pp. 153–156.
- [5] R. Kohno, H. Imai, M. Hatori, and S. Pasupathy, "Combination of an adaptive array antenna and a canceller of interference for direct-sequence spread-spectrum multiple-access system," *IEEE J. Select. Areas Commun.*, vol. 8, pp. 641–649, May 1990.
- [6] R. Kohno, P. B. Rapajic, and B. S. Vucetic, "An overview of adaptive techniques for interference minimization in CDMA systems," *Wireless Personal Commun.*, vol. 1, pp. 3–21, 1994.
- [7] M. D. Zoltowski and J. Ramos, "Blind adaptive beamforming for CDMA based PCS/cellular," in *Conf. Rec. 29th Asilomar Conf. Signals, Syst., Comput.*, Nov. 1995, pp. 378–382.
- [8] J. F. Ramos and M. D. Zoltowski, "Blind 2D RAKE receiver for CDMA incorporating code synchronization and multipath time delay estimation," in *Proc. Int. Conf. Acoust., Speech, Signal Process.*, vol. 5, Munich, Germany, Apr. 1997, pp. 4025–4028.
- [9] M. D. Zoltowski, Y.-F. Chen, and J. Ramos, "Blind 2D RAKE receivers based on space-time adaptive MVDR processing for the IS-95 CDMA system," in *Proc. Milcom.*, vol. 2, McLean, VA, Oct. 1996, pp. 618–622.
- [10] H. Liu and M. D. Zoltowski, "Blind equalization in antenna array CDMA systems," *IEEE Trans. Signal Processing*, vol. 45, pp. 161–172, Jan. 1997.
- [11] M. D. Zoltowski and J. Ramos, "Blind 2D RAKE receivers based on space-time MVDR processing," in *Interference Rejection and Signal Separation in Wireless Communications Symposium (IRSS '96)*. Newark, NJ, Mar. 1996.
- [12] T. F. Wong, T. M. Lok, J. S. Lehnert, and M. D. Zoltowski, "A linear receiver for direct-sequence spread-spectrum multiple access systems with antenna arrays and blind adaptation," *IEEE Trans. Inform. Theory*, vol. 44, pp. 659–676, Mar. 1998.
- [13] M. D. Zoltowski and J. Ramos, "Blind multi-user access interference cancellation for CDMA based PCS/cellular using antenna arrays," in *Proc. IEEE Int. Conf. Acoust., Speech, Signal Process.*, vol. 5, May 1996, pp. 2730–2733.
- [14] J. Ramos and M. D. Zoltowski, "Reduced complexity blind 2D RAKE receiver for CDMA," in *Proc. Eighth IEEE Signal Process. Workshop Stat. Signal Array Process.*, Corfu, Greece, June 1996, pp. 502–505.
- [15] J. Proakis, *Digital Communications*. New York: McGraw-Hill, 1992.
- [16] S. Verdu, "Minimum probability of error for asynchronous Gaussian multiple-access channels," *IEEE Trans. Inform. Theory*, vol. IT-32, pp. 85–96, Jan. 1986.
- [17] R. Lupas and S. Verdu, "Linear multiuser detectors for synchronous code-division multiple-access channels," *IEEE Trans. Inform. Theory*, vol. 35, pp. 123–136, Jan. 1989.
- [18] U. Madho and M. Honig, "MMSE interference suppression for direct-sequence spread spectrum CDMA," *IEEE Trans. Commun.*, vol. 42, pp. 3178–3188, Dec. 1994.
- [19] S. L. Miller, "An adaptive direct-sequence code-division multiple-access receiver for multiuser interference rejection," *IEEE Trans. Commun.*, vol. 43, pp. 1746–1754, Feb. 1995.
- [20] A. Paulraj, B. Khalaj, and T. Kailath, "2-D RAKE receivers for CDMA cellular systems," in *Proc. IEEE GLOBECOM*, vol. 1, San Francisco, CA, Dec. 1994, pp. 400–404.
- [21] J. F. Ramos and M. D. Zoltowski, "Blind 2D RAKE receiver for CDMA incorporating code synchronization and multipath time delay estimation," in *Proc. First IEEE Signal Process. Workshop Signal Process. Adv. Wireless Commun.*, Paris, France, Apr. 1997, pp. 273–276.
- [22] TIA/EIA/IS-95, "Interim standard, mobile station-base station compatibility standard for dual mode wideband spread spectrum cellular system," in *Proc. Telecommun. Industry Assoc.*, Washington, DC, July 1993.
- [23] M. Wax and T. Kailath, "Detection of signals by information theoretic criteria," *IEEE Trans. Acoust., Speech, Signal Processing*, vol. ASSP-33, pp. 387–392, Apr. 1985.
- [24] T. S. Rappaport, S. Y. Seidel, and S. Yoshida, "900 MHz multipath propagation measurements for U.S. digital cellular radiotelephone," *Proc. IEEE*, vol. 77, pp. 84–89, Jan. 1989.



Javier Ramos received the B.Sc., M.Sc., and Ph.D. degrees from the Polytechnic University of Madrid, Madrid, Spain, in 1987, 1989, and 1995, respectively.

While pursuing the Ph.D. degree, he actively cooperated in several research projects at Purdue University, West Lafayette IN. In 1996, he was a Postdoctoral Research Associate at Purdue University. During 1997, he was an Assistant Professor at the Polytechnic University of Madrid. In 1998, he joined Carlos III University of Madrid, Leganés, Spain, where he is an Associate Professor. His areas

of research include third-generation mobile communications, array processing, digital communications, spread spectrum systems, and applications of GPS and cellular systems.

Dr. Ramos received the Ericsson Award for the best Ph.D. dissertation on digital communications in 1996.



Michael D. Zoltowski (F'99) was born in Philadelphia, PA, on August 12, 1960. He received the B.S. and M.S. degrees in electrical engineering with highest honors from Drexel University, Philadelphia, in 1983 and the Ph.D. degree in systems engineering from the University of Pennsylvania, Philadelphia, in 1986.

From 1982 to 1986, he was an Office of Naval Research Graduate Fellow. In the Fall of 1986, he joined the faculty of Purdue University, West Lafayette, IN, where he currently holds the position

of Professor of electrical and computer engineering. During 1987, he held the position of Summer Faculty Research Fellow at the Naval Ocean Systems Center, San Diego, CA. He is a contributing author to *Adaptive Radar Detection and Estimation* (New York: Wiley, 1991), *Advances in Spectrum Analysis and Array Processing, Vol. III* (Englewood Cliffs, NJ: Prentice-Hall, 1994), and *CRC Handbook on Digital Signal Processing*, (Boca Raton, FL: CRC, 1996). His present research interests include space-time adaptive processing and blind antenna array beamforming for all areas of mobile and wireless communications, radar, and GPS.

Dr. Zoltowski was the recipient of the IEEE Signal Processing Society's 1991 Paper Award in the statistical signal and array processing technical area. He received the "The Fred Eilersick MILCOM Award for Best Paper in the Unclassified Technical Program" at the IEEE Military Communications (MILCOM '98) Conference. He also received the IEEE Outstanding Branch Counselor Award for 1989–1990 and the Ruth and Joel Spira Outstanding Teacher Award for 1990–1991. He has served as an Associate Editor for the IEEE TRANSACTIONS ON SIGNAL PROCESSING and is currently an Associate Editor for the the IEEE COMMUNICATIONS LETTERS. Within the IEEE Signal Processing Society, he has been a member of the Technical Committee for the Statistical Signal and Array Processing Area and is currently a member of the Technical Committee for Communications and the Standing Committee on Education. In addition, he is currently a Member-at-Large of the Board of Governors and Secretary of the IEEE Signal Processing Society.

Hui Liu (S'92–M'96) received the B.S. degree in 1988 from Fudan University, Shanghai, China, the M.S. degree in 1992 from Portland State University, Portland, OR, and the Ph.D degree in 1995 from The University of Texas, Austin, all in electrical engineering.

During the summer of 1995, he was a consultant for Bell Northern Research, Richardson, TX. From June 1996 to December 1996, he served as Director of Engineering at Cwill Telecommunications, Inc. He held a position of Assistant Professor at the Department of Electrical Engineering, University of Virginia, Charlottesville, from September 1995 to July 1998. He is now with the Department of Electrical Engineering, University of Washington, Seattle. His current research interests include wireless communications, array signal processing, DSP and VLSI applications, and multimedia signal processing.

Dr. Liu is a member of the Radio Communications Committee (RCC) and the Signal Processing and Communication Electronics Committee (SPCE) and the IEEE Communications Society. He is a recipient of an 1997 NSF CAREER Award.